Journal of Microelectronics and Electronic Packaging (2009) **6**, 108-113

ISSN: 1551-4897

Fabrication and Testing of an LTCC Microfluidic Serial Dilution Device

Marcio Rodrigues da Cunha, Mario Ricardo Gongora-Rubio,* Izabela Dutra Alvim, and Maria Ines Ré

Abstract—**Usually in chemical and biotechnology laboratories, preparing liquid reagents and samples with distinctive concentrations is a basic process applied to all experiments. Most of the time, this process is done by manual pipetting whose accuracy and repeatability depend on the researcher's expertise. In addition, preparing reagents and samples is a time-consuming process, because of the amount of time needed for pipette regulation, suction, and infusion. Buffer solutions are solutions that resist change in hydronium ion and hydroxide ion concentration (and consequent pH) upon addition of small amounts of acid or base, or upon dilution. Their resistance to changes in pH makes buffer solutions useful for chemical and biochemical processes. A buffer of carbonic acid (H_2CO_3), bicarbonate (HCO_3^-), and phosphate ($H_2PO_4^-$) is present in blood plasma to maintain a pH between 7.35 and 7.45. Industrially, buffer solutions are used in fermentation processes and in setting in vivo conditions for biotechnological experiments, as well as in chemical analysis and calibration of pH meters. The present work reports the potential of 3D LTCC (Low Temperature Cofired Ceramics) to obtain microfluidic structures for the continuous production of buffer solutions with different pH levels. Design, device simulation, and fabrication as well as experimental results are presented.**

Keywords—**Buffer solutions, LTCC, microfluidic devices serial dilution**

Introduction

The uses of microfluidic devices have steadily increased for analytical chemistry and life science applications. The economic potential of microfluidic solutions is relevant to industry and applied research. Some examples of the use of this technology are DNA sequencing, sample preparation, microparticle production, cell separation, and so forth. This paper addresses the use of LTCC technology to obtain serial dilution microfluidic structures for continuous production of buffer solutions with different pH levels.

LTCC Technology for Microfluidics

Ceramic multilayer technology is widely used for aerospace, automotive, RF, microwave, and other high reliability applications with high packaging density needs. LTCC offers the benefit of straightforward fabrication, low cost processing, ruggedness, self-packaged devices and systems, and overall low cost. Initially, LTCC modules were only used for electrical functions [1, 2]. Such electronic LTCC modules consist of dielectric tapes, connecting vias, internal and external conductors, passive components (resistors, capacitors, and inductors), and external active devices as shown in Fig. 1.

The exceptional attributes of the LTCC material system and processes allowed for the integration of nonelectrical functions [3, 5, 6] such as microfluidic, photonic, mechatronic, microplasma, and microreaction to create microsystems for wireless networks, energy, chemical process industry, and life science applications.

Dilutions in Chemical and Biochemical Procedures

Performing chemical or biochemical analysis, synthesis, or preparations, even at the most basic levels, requires carrying out a large number of separate manipulations on the material components, including measuring, transferring, concentrating, making aliquots, diluting, separating, detecting, and so on.

Although microfluidic technologies are being applied to some of these manipulations, there are still a number of areas where that application is not so straightforward. It would be desirable to provide microfluidic devices that are capable of performing each of the various manipulations required for in situ dilution or concentration of a particular material within a microfluidic format.

Serial dilution is a technique for creating different concentrations of a sample where the concentration will be decreased. In general, this process is done manually with pipette processes whose tolerance depends mainly on the skill of the technician handling the pipette tools with sample solutions, as shown in Fig. 2. In addition, conventional serial dilution is a time-consuming process due to its inefficiency.

The dilution factor (*DF*) is defined as:

$$DF = \frac{Vol_{\text{sample}}}{Vol_{\text{total}}} = \frac{Vol_{\text{sample}}}{Vol_{\text{sample}} + Vol_{\text{buffer}}} \quad (1)$$

where Vol_{sample} is the volume of the sample, Vol_{total} is the total volume, and Vol_{buffer} is the volume of the buffer. Serial dilutions are dilutions made from dilutions, so the serial dilution factor is just the product of the individual dilution factors.

$$DF_{\text{serial}} = DF_1 \times DF_2 \quad (2)$$

Several researchers have investigated serial dilution devices using microfluidic techniques. In Bang et al. [7] the serial dilution

Manuscript received October 2008 and accepted June 2009
Institute for Technological Research of the State of São Paulo, Technological Center for Processes and Products, Cidade Universitária, CEP 05508-901 São Paulo/SP, Brazil
*Corresponding author; e-mail: gongoram@ipt.br

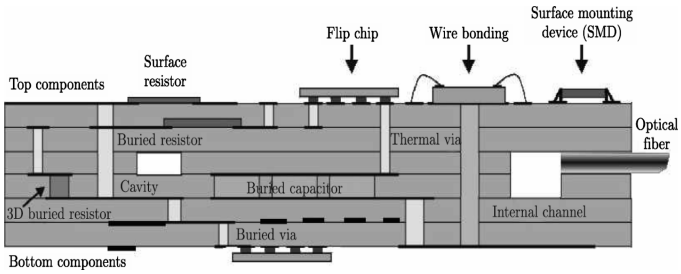

Fig. 1. Typical LTCC module [5].

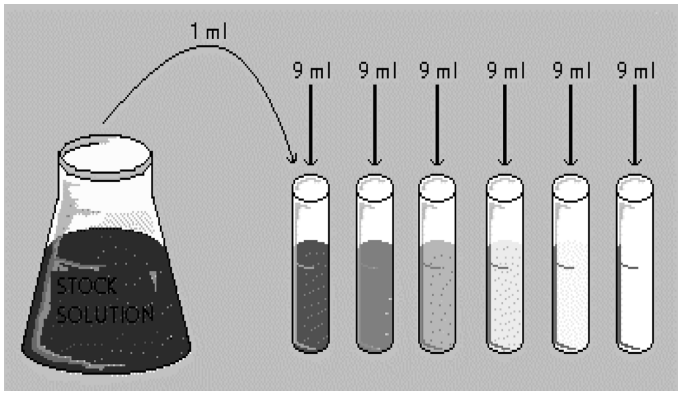

Fig. 2. Manual serial dilution.

mechanism of the microchip is performed simply in that the number of microchannels with the same flow rate determines the total amount of flow into the wells, as shown in Fig. 3.

This approach ensures the reproducible function of the device; microchannels of the chip were fabricated by PDMS and have a tetragonal cross section with a length of 50 μm of each side.

Another interesting application describes a miniaturized, microfluidic version of a serial-dilution fluorescent immunoassay [8]. This PMDS assay is capable of analyzing multiple antibodies quantitatively and in parallel in small volumes of liquids in one experiment, as shown in Fig. 4.

A network approach for generating serial dilutions is presented in Walker et al. [9] in which a device with two PDMS layers was constructed and dilutions are created to be independent of the flow rate through the device. The only requirement is that the flow rate and viscosity of each fluid input are the same.

The design is composed of two functionally equivalent branch networks, one mirrored and superimposed upon the other in a stacked two layer structure, with the branch ends meeting at common outlets, see Fig. 5. The branch resistances from each manifold are matched such that the combined flow rates always sum to unity.

Most of serial dilution implementations are in PDMS, which prevents serial dilution at high temperatures and with some industrial solvents.

Serial Dilution in LTCC

Our method takes advantage of the 3D structure capabilities of LTCC. Microfluidic devices for serial dilution were designed for generating different dilution factors for the continuous production of buffer solutions with different pH values.

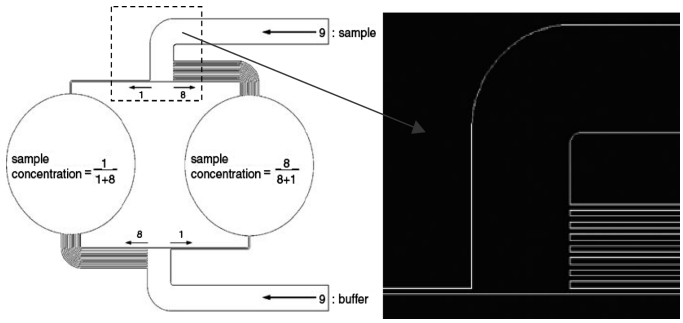

Fig. 3. Serial dilution with microchannels [7].

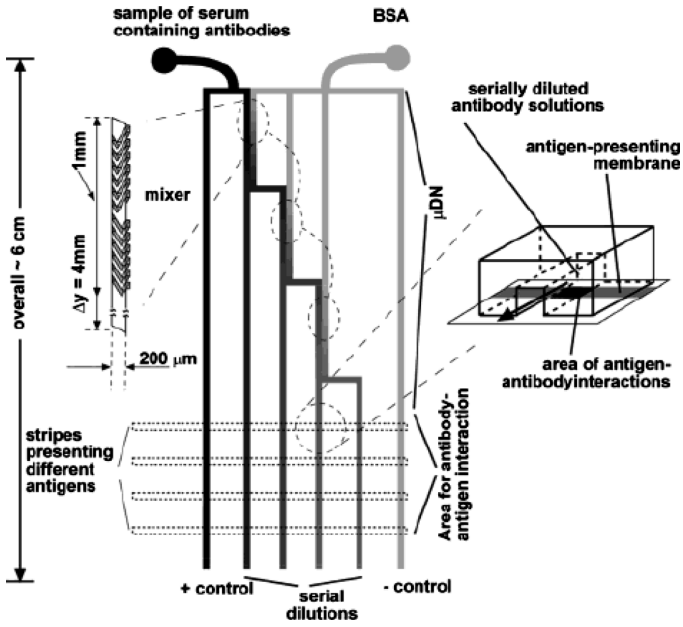

Fig. 4. Serial dilution immunoassay [8].

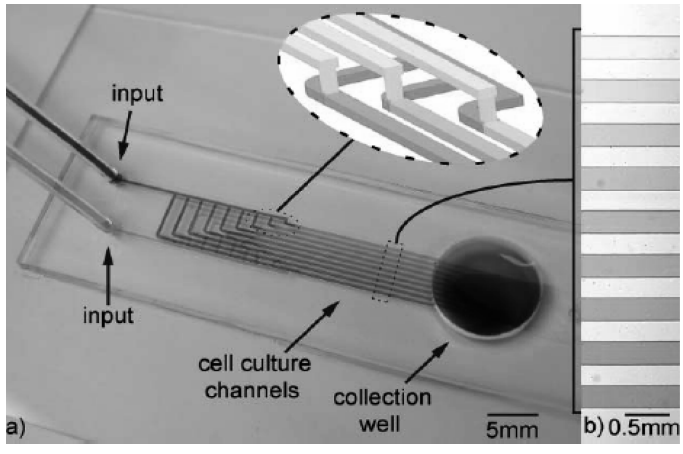

Fig. 5. Serial dilution using a network approach [9].

A. Microfluidic Device Fabrication

LTCC green tapes are glass-ceramic composite materials commercially produced in flat tapes of various thicknesses, usually in the range of 100-300 μm.

The processing of the green ceramic tapes was done in four basic steps [4]:

1. An AutoCAD software tool was used to design fluidic structures of each green tape layer.
2. Each individual layer was patterned using a CO_2 laser.
3. The tapes were collated and laminated under pressure and temperature.
4. The entire laminate was cofired to sinter the material.

The microfluidic devices were fabricated in LTCC. The green tape used in this work was 250 mm thickness LTCC 951AX from DuPont (Towanda Plant, PA). The lamination step was carried out at 80°C under a pressure of approximately 200 kgf/cm^2 for 30 min. Green tapes were machined using a commercial 40 W CO_2 Versa Laser VL 300 (Scottsdale, AZ) with a special high power density focusing optics fixture.

B. Buffer Solutions Device

Two microfluidic devices for buffer solution generation were fabricated and tested. The designed devices were intended to generate nonlinear dilutions. In the present work we chose some physiological media to generate five different pH values (see Table III, discussed below).

The first device (BS-1) is a linear microchannel array that includes two sections, shown in blue and green in Fig. 6(a) with microchannels merged into an output chamber (red) to obtain buffer solution outputs. Each section defines flow rates for sample or buffer solutions in order to obtain specific volumes for dilutions using different hydraulic resistances.

The second device (BS-2) was fabricated after the BS-1 device was tested [11], and is composed of a microchannel circular array that includes two sections, shown in blue and green in Fig. 6(b) and at the mixer stage after flow merge vias. An outline of the fabricated devices is shown in Fig. 7(a) (BS-1) and Fig. 7(b) (BS-2) with epoxy bonded brass input flanges.

A photograph of the LTCC machined section 1 of the BS-1 device with channel identification is shown in Fig. 8(a). Channel T1 provided access for the sample solution, and channels A and B distributed the solution for dilution channels 1a to 5a. LTCC machined section 2 with channel identification can be seen in Fig. 8(b). Channel T2 provided access for the buffer solution, and channels C and D distributed solutions for dilution channels 1b to 5b.

Computational Model

Simulations were carried using finite element software (COMSOL 3.3). The module used for simulation of the structures was the Incompressible Navier-Stokes module in the laminar and permanent regimen. Numerical simulation work was divided into two stages: calculation of the hydraulic resistance, and structures 1 and 2 of BS-1 device, shown in blue and green in Fig. 6(a). A typical mesh arrangement for simulated structures is shown in Fig. 9.

A. Calculation of the Hydraulic Resistance

Given Hagen-Poiseuille laminar flow conditions, the volume flow rate in a microchannel is given by eq. (3).

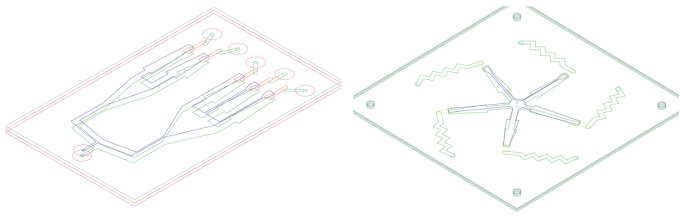

(a) (b)

Fig. 6. Geometry of buffer solutions devices (a) BS-1 and (b) BS-2.

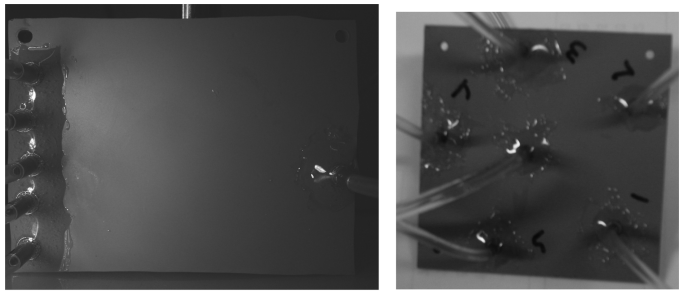

(a) (b)

Fig. 7. Fabricated microfluidic devices (a) BS-1 and (b) BS-2.

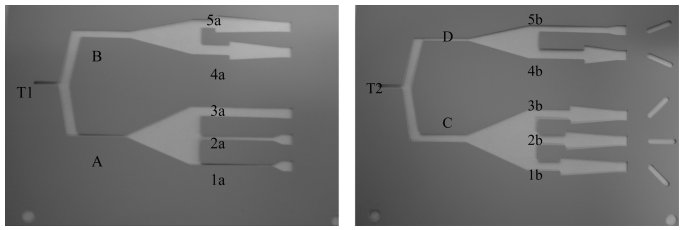

Fig. 8. BS-1 device sections 1 and 2.

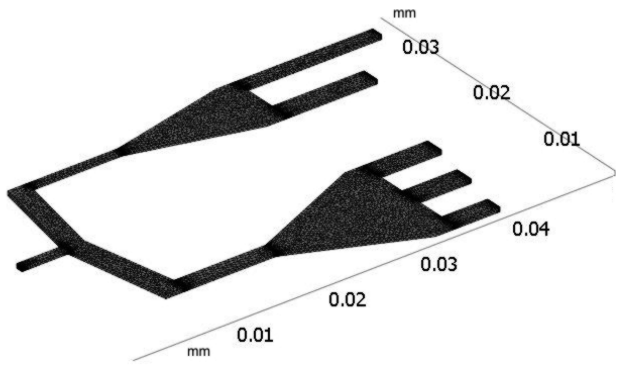

Fig. 9. The mesh used for section 2.

$$Q = \Delta P / R \tag{3}$$

Predefining flow rates and equalizing pressure drops for sample and buffer solutions, as shown in eq. (4), allows us to obtain the required hydraulic resistance ratio.

$$R_{\text{hyd1}} \cdot Q_1 = R_{\text{hyd2}} \cdot Q_2 \tag{4}$$

The rectangular microchannel model for hydraulic resistance obtained in Henrik [10] was adopted for calculation of the microchannel dimensions.

$$R_{\text{hyd}} = \frac{12\eta L}{wh^3} \cdot \left[1 - \frac{h}{w} \cdot \left(\frac{192}{\pi^5} \cdot \sum_{n=1,3,5}^{\infty} \frac{1}{n^5} \cdot \tanh\left(\frac{n\pi w}{2h}\right)\right)\right]^{-1} \quad (5)$$

In this work it is desired to implement a device that has well defined flow rates in the channels. At the basic principle level, the device had a defined pressure drop (ΔP) of 50 Pa for all channels and through the adjustment of the hydraulic resistances the desired flow rates were reached using eq. (3).

Fig. 10 illustrates the several hydraulic resistances used in the dilution devices project, showing mainly the geometric adjustments (length and cross section of the channels) to reach the desired flow rates.

Table I shows the results of the hydraulic resistances calculations, presenting the pressure drop (ΔP) applied in channels, the obtained flow rate (Q), the ratio between the flow rates of the desired channels (Q#/QT1, Q#/QA, Q#/Q1a), the target ratios, and the deviation between them.

Table I gives data verifying that the adjustment of the hydraulic resistances was successful, reaching simulated ratios with only minor standard deviations of 1%. Therefore, these results show that the device was implemented successfully.

B. Calculation of the Interconnection Structures 1 and 2

As will be seen in the Experimental Results section, we observed deviations from the simulated pH levels to those obtained experimentally. Therefore, further simulation was carried out in order to verify the influence of the coupling of several hydraulic resistances in the configuration of the dilution devices. For a more detailed study of deviations for the BS-1 device, structures 1 and 2 were been divided into three stages and simulated separately.

Fig. 11 shows structure 1 divided into three stages for verification of the variations found in the Experimental Results. Figs. 11(a), 11(c), and 11(e) show the pressure fields, demonstrating a disequilibrium in the pressure between the side with three channels and the side with two channels.

Table II shows the results obtained with the coupled hydraulic resistances. It is possible to observe that the coupling generated significant variation of ΔP at several resistances, thus influencing the flow rates obtained in each one of the channels, generating significant deviations between the target and the obtained flow rates ratio.

This disequilibrium in the pressure is due to a higher equivalent resistance in the three channels side. Figs. 11(b), 11(d), and 11(f) show the streamlines in the three stages, where it can be verified that the distribution of the flow rate was not the expected value due to a fluctuation in pressure, indicating a mismatch in the fabricated BS-1 device.

Experimental Results

Experimental tests were conducted to obtain buffer solutions. An experimental setup for testing was implemented using two syringe pumps followed by fluidic diodes in order to apply two saline solutions (Solution 1—monosodium phosphate, monohydrate; and Solution 2—disodium phosphate, heptahydrate) to the proper inlets of the microfluidic device under test. A pH meter was used to obtain the resultant data from the dilution outputs, as depicted in Fig. 12.

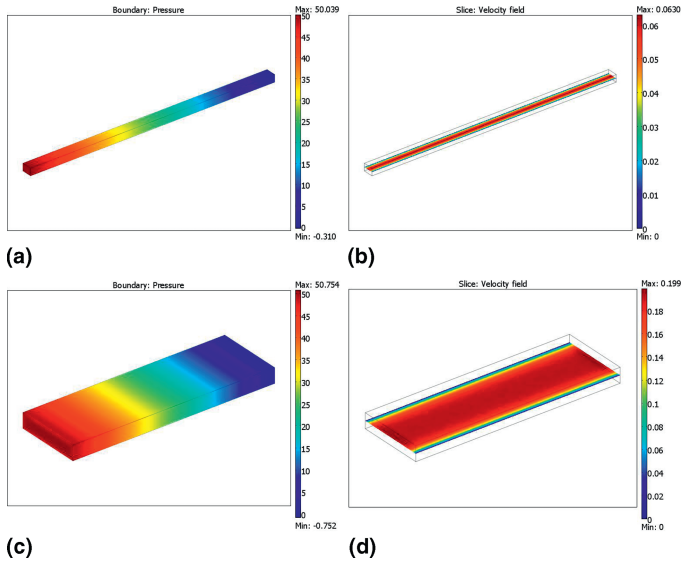

Fig. 10. Several hydraulic resistances used in the project.

Table I
Results of the Hydraulic Resistances Adjusted for Formation of Dilution Device

Channels	ΔP	Q#	Q#/QT1	Target	Deviation
T1	49.83	1.54	1.00	1.00	0.00
T2	49.81	1.92	1.25	1.25	0.16
Channels	ΔP	Q#	Q#/QA	Target	Deviation
A	49.91	0.37	1.00	1.00	0.00
B	49.90	2.05	5.60	5.61	−0.18
C	49.89	2.37	6.47	6.49	−0.32
D	49.90	0.65	1.78	1.78	0.25
Channels	ΔP	Q#	Q#/Q1a	Target	Deviation
1a	49.97	0.02	1.00	1.00	0.00
2a	49.94	0.47	30.90	30.78	0.39
3a	49.93	2.01	132.33	132.39	−0.04
4a	49.84	5.25	345.73	344.39	0.39
5a	49.66	8.82	580.88	576.33	0.78
1b	49.80	5.84	384.63	382.83	0.47
2b	49.68	5.69	374.88	367.50	1.97
3b	49.87	4.80	316.04	315.17	0.28
4b	49.90	3.13	206.36	206.00	0.17
5b	49.94	1.32	86.69	86.56	0.15

Buffer solutions are solutions that resist change in hydronium ion and hydroxide ion concentration (and consequently pH) upon addition of small amounts of acid or base, or upon dilution.

Their resistance to changes in pH makes buffer solutions very useful for chemical and biochemical processes. A buffer of carbonic acid (H_2CO_3), bicarbonate (HCO_3^-), and phosphate ($H_2PO_4^-$) is present in blood plasma in order to maintain a pH between 7.35 and 7.45.

The designed microfluidic devices were specified to give five different mixtures of salt solutions, and consequently, five different pH levels. Table III presents the chosen pH levels and their importance in laboratory and industry procedures.

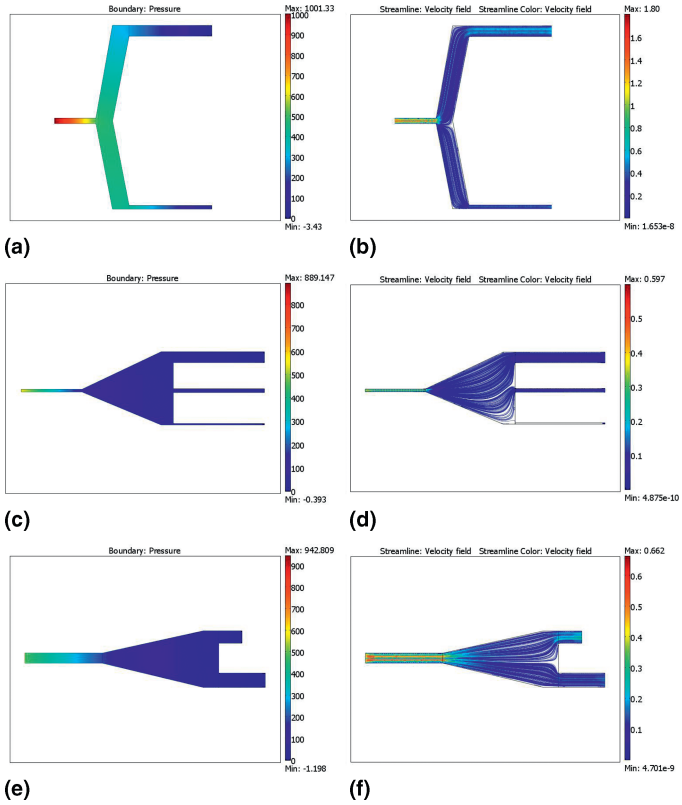

Fig. 11. Structure 1 divided into three stages.

Table II
Results of the Hydraulic Resistances After the Division of the Structures in Stages

Channels	ΔP	Q#	Q#/QT1	Target	Deviation
T1	491.93	14.57	1.00	1.00	0.00
T2	481.74	18.00	1.24	1.25	−1.15
Channels	ΔP	Q#	Q#/QA	Target	Deviation
A	418.63	3.020	1.00	1.00	0.00
B	287.64	11.89	3.94	5.61	−42.54
C	276.87	13.26	4.39	6.49	−47.78
D	392.801	5.10	1.69	1.78	−5.45
Channels	ΔP	Q#	Q#/Q1a	Target	Deviation
1a	69.23	0.01	1.00	1.00	0.00
2a	66.35	0.61	44.53	30.78	30.87
3a	59.61	2.41	177.42	132.39	25.38
4a	47.44	5.00	367.50	344.39	6.29
5a	39.38	6.98	512.90	576.33	−12.37
1b	37.34	4.38	322.04	382.83	−18.88
2b	42.70	4.78	351.13	367.50	−4.66
3b	40.45	3.90	286.82	315.17	−9.88
4b	54.30	3.42	251.37	206.00	18.05
5b	58.80	1.55	113.96	86.56	24.05

After initial tests were applied to the fabricated device, solutions of monosodium phosphate (monohydrate, 5% w/v) and disodium phosphate (heptahydrate, 5% w/v) were added in order to obtain the desired pH values. The amount of each salt was added in distilled water, under magnetic stirring, until

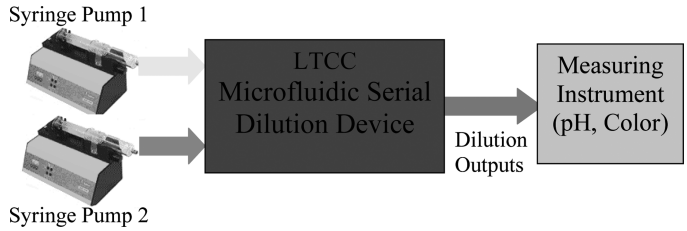

Fig. 12. Experimental apparatus.

Table III
Some Physiological Media and their Respective pH Levels

Medium	pH	Test pH
Blood	7.3-7.5	7.4
Intracellular ambient	6.6-7.0	6.8
Intestine	6.0-8.0	7.4
Nasal mucus	5.0-6.7	5.5 and 6.2
Inhibition of toxins production by Clostrídio botulinum in food	<4.5	4.5
Stomach	1.2-2.0	—

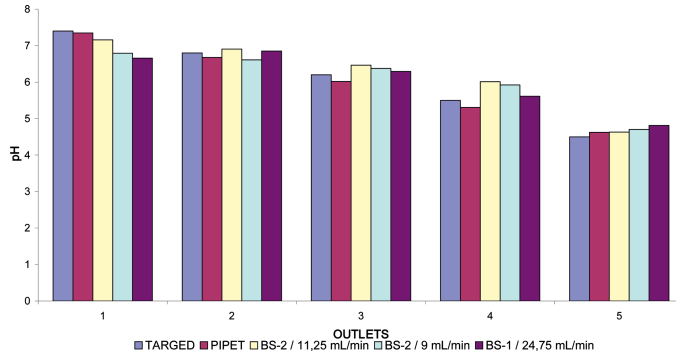

Fig. 13. Comparison between the theoretical and experimental values of pH levels.

complete dissolution. Each mixture was produced five times and the pH was measured using a pH meter model MP-225 (Metler-Toledo, Greinfensee, Switzerland) instrument previously calibrated with standard solutions.

As shown in Fig. 13, a comparison between the theoretical and experimental values (manual and continuous) of pH levels obtained is presented. Target values determined the device design parameters such as flow rate in each channel. The solutions were manually prepared with pipettes. The BS-2 LTCC microfluidic device was tested at different pumping rates of 9 mL/min and 11.25 mL/min; and the BS-1 device was tested at 24.75 mL/min.

Table IV gives the experimental pH values and standard deviations for the different device outlets. In manual (pipette) preparation of buffer solutions that display deviations, pH adjustment was completed by adding solution components until the target value was attained.

Some experimental deviations are apparent, but in spite of these deviations the evaluated devices (BS-1 and BS-2) presented good repeatability as the standard deviation results certify.

Table IV
pH Results and Standard Deviations for Fabricated Devices

Target (pH)		7.4(1*)	6.8(2)	6.2(3)	5.5(4)	4.5(5)
	(pH)	7.35	6.68	6.02	5.31	4.62
Pipette	SD	0.021	0.015	0.020	0.017	0.040
	(pH)	7.16	6.91	6.46	6.01	4.63
BS-2, 11.25 mL/min	SD	0.056	0.080	0.146	0.197	0.029
	(pH)	6.79	6.61	6.38	5.92	4.70
BS-2, 9 mL/min	SD	0.071	0.015	0.064	0.017	0.047
	(pH)	6.66	6.85	6.29	5.62	4.81
BS-1, 24.75 mL/min	SD	0.024	0.045	0.005	0.134	0.288

*Values in parentheses indicate number of outlets.

Conclusions

The fabrication of a LTCC microfluidic device for the production of buffer solutions with different pH was described. We believe that due to dimensional problems in device microchannels, a mismatch of hydraulic resistance caused a flow rate error to appear in channel structures, changing the outlet pH. Further work in order to optimize dimensional control of microfluidic structures is ongoing.

The continuous preparation of buffer solutions is feasible, opening perspectives for other laboratorial applications such as standard curve preparations, cytotoxicity, and microbiology experiments.

The current direction of the present research is oriented to obtain a microsystem that can control pH by inclusion of sensors (ISFET sensor) and micropumps to dynamically correct pH levels.

Acknowledgments

The authors thank CNPq and FAPESP for partial financial support.

References

[1] A.L. Eustice, S.J. Horowitz, J.J. Stewart, A.R. Travis, and H.T. Sawhill, "Low-temperature co-fired ceramics: A new approach to electronic packaging," in Proceedings of the 36th Electronic Components Conference, pp. 37-67, 1986.

[2] H.C. Bhedwar and H.T. Sawhill, "Ceramic multilayer package fabrication," Packaging, pp. 460-469, 1990.

[3] M.R. Gongora-Rubio, P. Espinoza-Vallejos, L. Sola-Laguna, and J.J. Santiago-Aviles, "Overview of low temperature co-fired ceramics tape technology for meso-system technology," Sensors and Actuators A: Physical, Vol. 89, pp. 222-241, 2001.

[4] Dupont Microcircuit Materials, "Dupont green tape material system design and layout guidelines" 2003, http://www2.dupont.com/MCM/en_US/products/green_tape/green_tape_index.html.

[5] L.J. Golonka, "Technology and applications of low temperature cofired ceramic (LTCC) based sensors and microsystems," Bulletin of the Polish Academy of Sciences: Technical Sciences, Vol. 54, No. 2, pp. 221-231, 2006.

[6] K.A. Peterson, S.B. Rohde, C.A. Walker, K.D. Patel, T.S. Turner, and C.D. Nordquist, "Micro-system integration with new techniques in LTCC," in Proceedings of IMAPS Conference and Exhibition on Ceramic Interconnect Technology, pp. 19-26, 2004.

[7] H. Bang, S.H. Lim, Y.K. Lee, S. Chung, C. Chung, D.-C. Han, and J.K. Chang, Serial dilution microchip for cytotoxicity test, *Journal of Micromechanics and Microengineering*, Vol. 14, pp. 1165-1170, 2004.

[8] X. Jiang, J.M.K. Ng, A.D. Stroock, S.K.W. Dertinger, and G.M. Whitesides, "A miniaturized, parallel, serially diluted immunoassay for analyzing multiple antigens," *Journal of the American Chemical Society*, Vol. 125, No. 18, pp. 5294-5295, 2003.

[9] M.G. Walker, N. Monteiro-Riviere, J. Rouse, and A.T. O'Neill, "A linear dilution microfluidic device for cytotoxicity assays," *Lab on a Chip*, Vol. 7, pp. 226-232, 2007.

[10] B. Henrik, "*Theoretical Microfluidics*," Lecture Notes, 2nd ed., Department of Micro and Nanotechnology, Technical University of Denmark, 2005.

[11] M. Rodrigues da Cunha, M.R. Gongora-Rubio, I.D. Alvim, and M.I. Ré, "Fabrication and testing of a LTCC microfluidic serial dilution device," in Proceedings of IMAPS/ACerS 4th International Conference and Exhibition on Ceramic Interconnect and Ceramic Microsystems Technologies (CICMT-2008), 2008.